



Microstructure and tribological performance of self-lubricating diamond/tetrahedral amorphous carbon composite film

Xinchun Chen, Zhijian Peng*, Xiang Yu, Zhiqiang Fu, Wen Yue, Chengbiao Wang

School of Engineering and Technology, China University of Geosciences, Beijing 100083, PR China

ARTICLE INFO

Article history:

Received 20 August 2010

Accepted 28 October 2010

Available online 18 November 2010

PACS:

81.05.Uw

Keywords:

Self-lubricating

Diamond

Tetrahedral amorphous carbon

Composite film

ABSTRACT

In order to smooth the rough surface and further improve the wear-resistance of coarse chemical vapor deposition diamond films, diamond/tetrahedral amorphous carbon composite films were synthesized by a two-step preparation technique including hot-filament chemical vapor deposition for polycrystalline diamond (PCD) and subsequent filtered cathodic vacuum arc growth for tetrahedral amorphous carbon (ta-C). The microstructure and tribological performance of the composite films were investigated by means of various characterization techniques. The results indicated that the composite films consisted of a thick well-grained diamond base layer with a thickness up to 150 μm and a thin covering ta-C layer with a thickness of about 0.3 μm , and sp^3 -C fraction up to 73.93%. Deposition of a smooth ta-C film on coarse polycrystalline diamond films was proved to be an effective tool to lower the surface roughness of the polycrystalline diamond film. The wear-resistance of the diamond film was also enhanced by the self-lubricating effect of the covering ta-C film due to graphitic phase transformation. Under dry pin-on-disk wear test against Si_3N_4 ball, the friction coefficients of the composite films were much lower than that of the single PCD film. An extremely low friction coefficient (~ 0.05) was achieved for the PCD/ta-C composite film. Moreover, the addition of Ti interlayer between the ta-C and the PCD layers can further reduce the surface roughness of the composite film. The main wear mechanism of the composite films was abrasive wear.

© 2010 Elsevier B.V. All rights reserved.

1. Introduction

The unique properties of diamond are promising for extensive applications in many fields of industry. In particular, in cutting tool protection [1–3], diamond films have been used as anti-abrasion components because of their high hardness, excellent wear resistance and chemical inertness. However, traditional chemical vapor deposition (CVD) polycrystalline diamond (PCD) films usually have coarse surface (surface roughness R_a up to a few microns), with crystallinity, crystal size and grain orientation varied with deposition parameters [4]. High surface roughness will lead to higher friction coefficient and wear rates, deteriorating the tribological performance of diamond films. It is then of great interest to smooth the surface and further enhance the wear resistance property of diamond films.

In recent years, various methods for smoothing the surface of diamond films have been developed. Nanocrystalline diamond (NCD) film [5–7], diamond polishing [8], activated hydrogen etching on surface [9], substrate pretreatment [10], addition of

interlayers [11], growth parameters control [12], alternate deposition of poly/nanocrystalline diamond multilayer [13–15], and solid lubrication composite coating on diamond films [16], have been proved to be effective tools to lower the surface roughness and improve the tribological behavior of the diamond film.

Diamond-like carbon (DLC) films [17], a group of metastable amorphous carbon films rich in sp^3 bonds, have also shown excellent mechanical properties and tribological performance (low friction coefficient ~ 0.1). Especially tetrahedral amorphous carbon (ta-C), possessing high sp^3 -bond carbon fraction (up to 90%) and smooth surface ($R_a \sim 0.1 \text{ nm}$) [18], has extremely low friction coefficient (lower to 0.02) and wear rate ($\sim 10^{-9} \text{ mm}^3/\text{Nm}$) [19]. During friction and wear process, the ta-C film transforms by stress-induced transformation to graphitic over-layer, which can act as a solid wear-reducing lubricant [19]. In dry solid–solid friction, Nosonovsky and Bhushan [20] have reviewed that various types of inhomogeneities between the contacting bodies, including surface roughness, material deformation and contamination, lead to friction. Surface roughness is one of the major factors in determining frictional behavior. Every nominally flat surface is not ideally smooth and has roughness due to small asperities. A contact between the two bodies during friction occurs only at the summits of the asperities. The friction coefficient is not only a material property but also an indication of contact mechanics between surfaces

* Corresponding author. Tel.: +86 10 82320255; fax: +86 10 82322624.

E-mail addresses: pengzhijian@cugb.edu.cn, pengzhijian@tsinghua.org.cn (Z. Peng).

Table 1
The deposition parameters of two-step procedure for diamond/ta-C composite films.

HFCVD (first step for diamond deposition)		FCVA (second step for ta-C deposition)	
Parameters		Parameters	
CH ₄ /H ₂ flow (sccm)	3/150	Graphite cathode purity	99.99%
Reaction pressure (kPa)	5.5	Working pressure (Pa)	4.0×10^{-4}
Deposition temperature (K)	1073	Arc current (A)	55
Filament temperature (K)	2273 ± 50	Substrate temperature (K)	300
Bias current (A)	3.5	Bias voltage (V)	−100
Duration (h)	78	Deposition time (min)	60

with roughness. Thus, a very smooth surface is highly desirable to achieve excellent friction performance for most tribological applications. From this point of view, deposition of a lubricating ta-C layer (maintaining high hardness but with very smooth surface comparing to CVD diamond film) onto rough CVD polycrystalline diamond layer to form diamond/ta-C composite film may be an effective technique to lower the surface roughness of diamond film and achieve exceptional surface friction performance.

In the present work, a new set of self-lubricating diamond/ta-C composite films were prepared by a two-step procedure including first deposition of rough polycrystalline diamond layer by hot-filament chemical vapor deposition (HFCVD) and then tetrahedral amorphous carbon layer by filtered cathodic vacuum arc (FCVA). The microstructure and tribological performance of the as-deposited diamond/ta-C composite films were investigated.

2. Experimental details

2.1. Material preparation

Commercially available silicon carbide (SiC) wafers were selected as substrates. The SiC wafers were received with a mirror-like polished surface ($R_a = 0.025 \mu\text{m}$) and then were machined to the dimension of $20 \text{ mm} \times 20 \text{ mm} \times 9 \text{ mm}$ by laser cutting. The specimens were dipped in HF acid solution for 5 min to dissolve the oxides on the surfaces, and ultrasonically cleaned in acetone for 10 min to remove the surface contamination, followed by ultrasonically bathing in de-ionized water and drying by flowing air before deposition. The diamond/ta-C composite films were synthesized by a two-step procedure. Firstly, the polycrystalline diamond films were deposited in a HFCVD chamber. A gas mixture of methane and hydrogen was activated by four tungsten filaments (0.8 mm in diameter and 7.5 mm apart from each other) arranged in a 6 mm distance from the substrate. Then, the diamond-coated SiC specimens were enclosed in FCVA chamber for ta-C deposition. The carbon plasma was produced from the arc spot on a graphite cathode of 99.99% purity. The resulting plasma beam was then passed through an off-plane 90° bend solenoid to filter out particulates and other neutral species. To further lower the surface roughness of the diamond film, a $0.4 \mu\text{m}$ thick metal Ti interlayer was deposited onto the diamond surface prior to ta-C deposition. Thus, three groups of diamond films including single PCD diamond film, PCD/ta-C composite film, PCD/Ti/ta-C composite film were synthesized for comparison. The details of growth parameters were summarized in Table 1.

2.2. Sample characterization

The surface roughnesses of films were measured by a three dimensional white-light interfering surface profiler (Micro XAM-3D). FEI Quanta 200 FEG field emission scanning electron microscope (SEM) equipped with energy-dispersive X-ray spectroscopy (EDS) was used to investigate the microstructure and elemental composition of the as-deposited diamond films. Raman

measurements were performed with a Renishaw 2000 Raman spectrometer using a 514.5 nm line of Ar⁺ laser as the excitation wavelength. The X-ray diffraction (XRD) patterns were recorded by a Philips PW 1710 automated diffractometer, using glancing angle technique with an incidence angle of 2° . The carbon bonding of the diamond film was investigated by X-ray photoelectron spectroscopy (XPS, PHI Quantera SXM), using a single Al-K α X-ray source, operated at 250 W. A ball-on-disk tester (MS-T3000) was used to evaluate the tribological properties of the samples. The coated SiC specimens were fixed on a rotary platform with a sliding velocity of 0.125 m/s under a normal load of 5 N using a Si₃N₄ ball of 4 mm in diameter as the counterpart. The produced initial Hertzian contact pressure under this applied normal load was about 2.5 GPa. The duration was 8 h, equating to a sliding distance of 3600 m. The relative humidity during testing was $43 \pm 2\%$, and the temperature was $25 \pm 2^\circ\text{C}$. After the wear test, SEM observation and Raman measurements were carried out on the wear track to study the friction behavior and wear mechanism of the diamond films.

3. Results and discussion

3.1. Surface and fracture microstructure

The SEM surface morphologies of the three as-prepared samples are shown in Fig. 1 under different magnifications. For the single PCD film shown in Fig. 1a, it can be observed that an almost continuous coarse polycrystalline diamond film was obtained by HFCVD method. The crystal facets of the diamond film mainly exhibit (1 1 1) and (2 2 0) preferential orientation, with grain size in the range of 20–35 μm . The well-faceted diamond crystallites are surrounded by tiny ball-like diamond grains. These small-sized diamond crystallites may be formed due to the second re-nucleation during deposition. Moreover, the inset micrograph at high magnification clearly shows that some deep grooves existed between the well-faceted diamond crystallites, resulting in a relatively rough surface. It was measured by white-light interfering surface profiler that the surface roughness of the PCD film was up to $1.55 \mu\text{m}$. In comparison with PCD film, the PCD/ta-C composite film shown in Fig. 1b presents somewhat smoother surface. The diamond crystal facets and inter-crystal grooves are covered by the subsequently deposited ta-C film by FCVA, obtaining a surface roughness of $1.04 \mu\text{m}$. Especially for the PCD/Ti/ta-C composite film shown in Fig. 1c, the addition of Ti interlayer before ta-C deposition further smoothes the surface. The grooves are nearly filled in by Ti/ta-C composite layers as shown in the inset. The surface roughness R_a decreased to $0.73 \mu\text{m}$. Therefore deposition of covering material with superior smoothness (for example, ta-C, nanocrystalline diamond, and so on) onto rough polycrystalline diamond to form composite film is an effective tool to lower the surface roughness.

The SEM image of the cross-sectional fracture of typical PCD/Ti/ta-C composite film is presented in Fig. 2. It is clearly observed that the interface between SiC substrate and diamond film is relatively sharp and smooth. The polycrystalline diamond

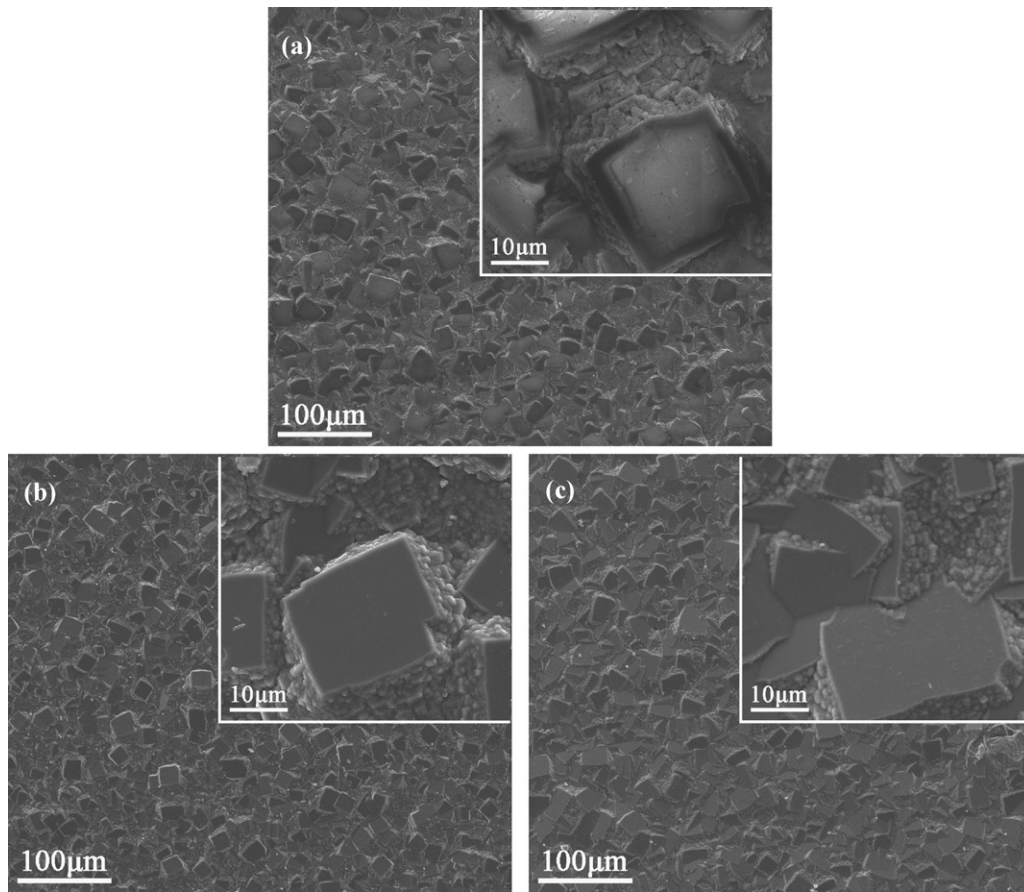


Fig. 1. SEM surface morphology of the as-deposited film samples: (a) PCD film, (b) PCD/ta-C composite film, and (c) PCD/Ti/ta-C composite film.

grown on SiC substrate exhibited a columnar structure along the deposition direction. It was measured by SEM that the thickness of the PCD film is approximately 150 μm . Thus, the mean growth rate for this HFCVD diamond film was approximately 1.92 $\mu\text{m}/\text{h}$. The top-most surface of the PCD/Ti/ta-C composite film was magnified to investigate the interfaces between neighboring layers. The magnified micrograph shows that Ti interlayer could successively grow over the PCD layer, and then ta-C layer succeeded in deposition onto the Ti interlayer. The Ti interlayer also has a columnar structure, and the top ta-C layer possesses a typical amorphous form. More importantly, uniform interfaces between each layer and smooth surface of the top ta-C layer were observed. The thicknesses of the Ti interlayer and the top ta-C layer are about 0.4 and 0.3 μm , respectively.

3.2. Crystallinity and chemical composition

The grazing incidence XRD patterns of the three film samples are illustrated in Fig. 3. The patterns show identical diamond peaks appeared at diffraction angle 2θ of 43.9° and 75.3° , which correspond to $\langle 111 \rangle$ and $\langle 220 \rangle$ reflections of diamond, respectively. According to the relative intensity of the $\langle 220 \rangle$ peak, the HFCVD-grown diamond has a predominant texture in $\langle 220 \rangle$ reflection. This gives evidences that the synthesized PCD films are composed of diamond crystallites. For PCD/ta-C and PCD/Ti/ta-C composite films, the intensities of the two diamond peaks decreased in sequence because the covering ta-C layer or Ti/ta-C layers weakened the incidence X-ray signal into the PCD layer. From Fig. 3, it can also be found that three metallic titanium diffraction peaks, $\langle 100 \rangle$, $\langle 002 \rangle$

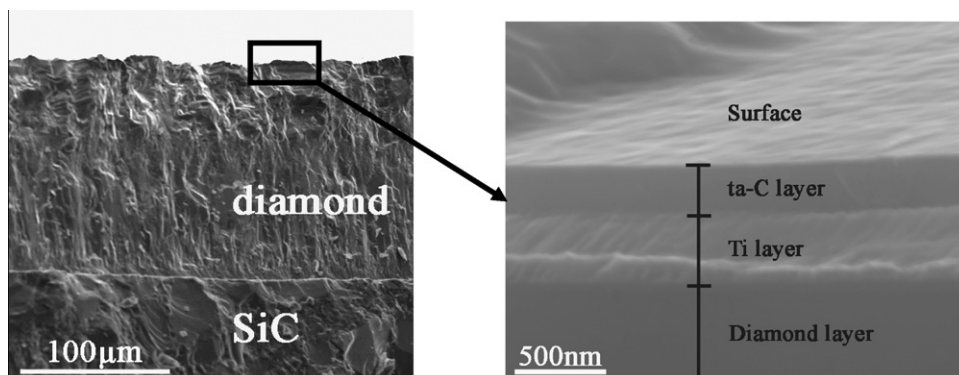


Fig. 2. Cross-sectional SEM image of the PCD/Ti/ta-C composite film.

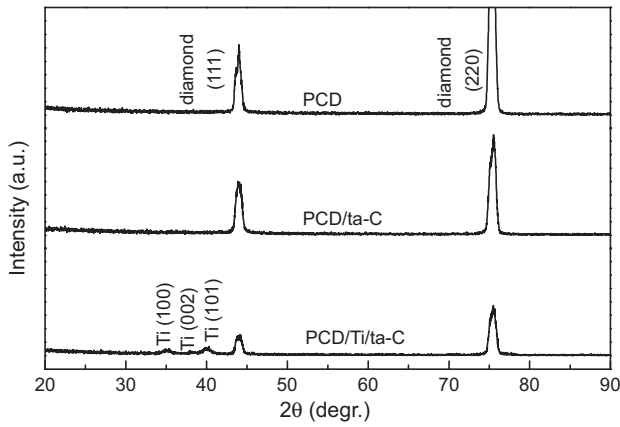


Fig. 3. Grazing incidence X-ray diffraction patterns of the as-deposited film samples.

and (101) reflections, are visible in PCD/Ti/ta-C composite film. These peaks were stemmed from the Ti interlayer.

Fig. 4 shows typical Raman spectra of the three as-prepared film samples on SiC substrate. A sharp peak appears at about 1332.7 cm^{-1} for the PCD film, which is the characteristic of diamond [21]. In addition, the PCD film contains non-diamond carbon phase, as suggested by the broad peak at $\sim 1562.7\text{ cm}^{-1}$. The presence of such a broad peak appearing at $\sim 1560\text{ cm}^{-1}$ can be taken as evidence of graphite-like sp^2 carbon structure [21,22]. Except for UV excitation, the Raman scattering factor for sp^2 sites is dozens of times higher than that of the sp^3 sites. Thus, given the sharpness of the diamond peak at 1332.7 cm^{-1} , it can be assumed that the PCD films are mainly composed of superior diamond crystallites in quality. For the PCD/ta-C composite film, the covering ta-C layer weakened the Raman scattering signal from the diamond layer, and simultaneously the broad peak at 1562.7 cm^{-1} becomes sharper, which was attributed to the increasing amount of the amorphous ta-C structure in the film. Moreover, the diamond peak at 1332.7 cm^{-1} has disappeared due to the addition of Ti interlayer for the PCD/Ti/ta-C composite film, which was caused by the high reflectivity of metal Ti to Raman visible excitation signal.

XPS analysis was carried out to get information of stoichiometry and bonding configurations of the ta-C film. Fig. 5 shows the Gaussian–Lorentzian fitting curve of C1s XPS result for the PCD/ta-C composite film. The deconvoluted peaks were located at 284.7 eV, 285.3 eV and 286.1 eV, which are assigned to sp^2 -C, sp^3 -C and C–O bonds, respectively. The reason for oxygen contaminant may be due to the prolonged exposure of the sample to the ambient atmo-

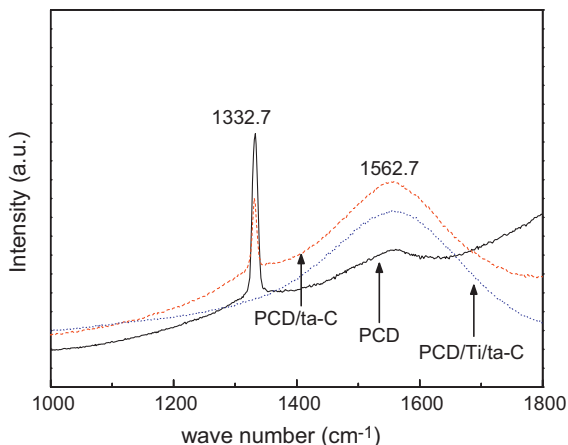


Fig. 4. Raman spectra obtained for the three as-deposited film samples.

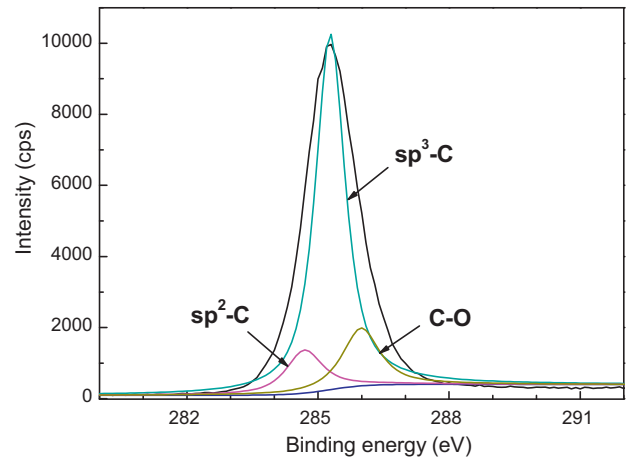


Fig. 5. Gaussian–Lorentzian fitted C1s XPS result for the covering ta-C layer measured on the PCD/ta-C composite film.

sphere. As it can be observed from Fig. 5, the shape of the C1s peak was mainly determined by the sp^3 -C peak, indicating that the sp^3 fraction of carbon atoms in the ta-C film is very high. It was calculated by the peak area that the sp^3 -C content in the ta-C film came up to 73.93%. The hardness of this synthesized ta-C film is among 71–80 GPa, reported elsewhere [23].

3.3. Tribological performance

Fig. 6 shows typical friction curves of the three as-grown samples on SiC substrates as a function of the duration time. As can be observed from this figure, the three samples have similar friction coefficient curve shape. The whole friction process can be divided into three distinct regimes, initial running-in stage, transition process and steady state. During the initial running-in stage (regime I, 0–20 min), the intense mechanical interactions between the sharp diamond asperities and the counterpart surfaces [24] resulted in an initial maximum friction coefficient ~ 0.55 . Then the friction coefficient immediately dropped to ~ 0.1 and fluctuated around this value. This typical friction stage of CVD-deposited polycrystalline diamond was also observed in previous works [25,26]. The subsequent transition process (regime II, 20–120 min) shows a first slight increase in friction coefficient, which was resulted from the increasing fragmentation and deformation of contacting asperities due to prolonged friction duration. And then the friction coefficient

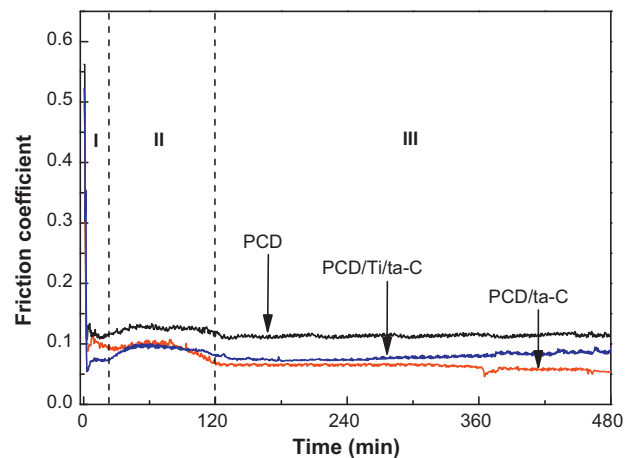


Fig. 6. Friction coefficient of the three as-deposited film samples sliding against Si_3N_4 ball.

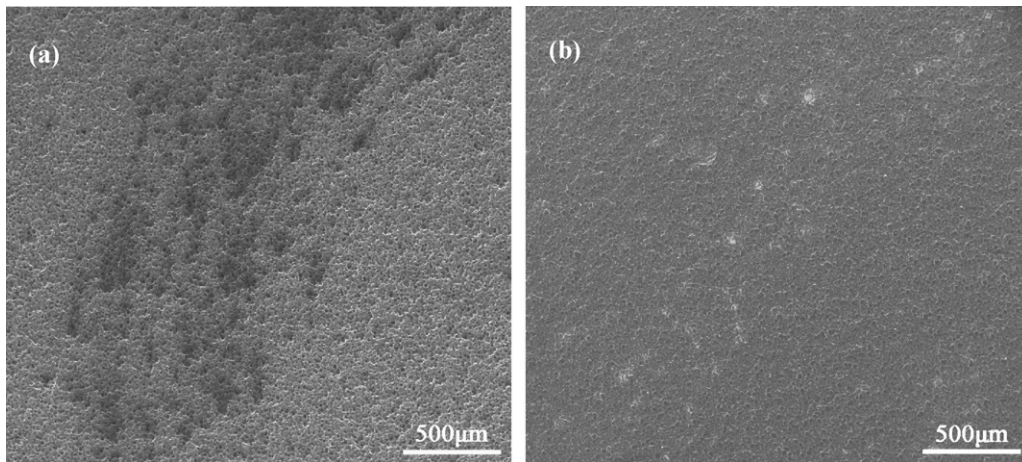


Fig. 7. Typical wear track after the wear test: (a) PCD film, (b) PCD/ta-C composite film.

gradually decreased because of the gradual blunting of asperities. Afterwards, entering the steady state (regime III, 120–480 min), the friction coefficient reached a steady value and remained stable for the rest duration of tests. As expected, the single PCD film exhibited a relatively high steady-state friction coefficient ~ 0.13 . In comparison with single PCD film, the composite films have much lower friction coefficient in steady state. In particular, for the PCD/ta-C composite film in steady state, the friction coefficient shows a reducing trend with increasing duration time. An

extremely low friction value ~ 0.05 was achieved at the end of the test. This friction-reducing phenomenon can be explained from two sides. Firstly, the decreased surface roughness of the composite film favored the reducing friction coefficient. Secondly, the friction-reducing was attributed to the lubricating effect of the ta-C film (see Raman results discussed in Fig. 10). It should be noted that the steady-state friction coefficient of the smoother PCD/Ti/ta-C composite film is a little higher than that of the PCD/ta-C composite film. Moreover, the friction coefficient shows a slight increase with the

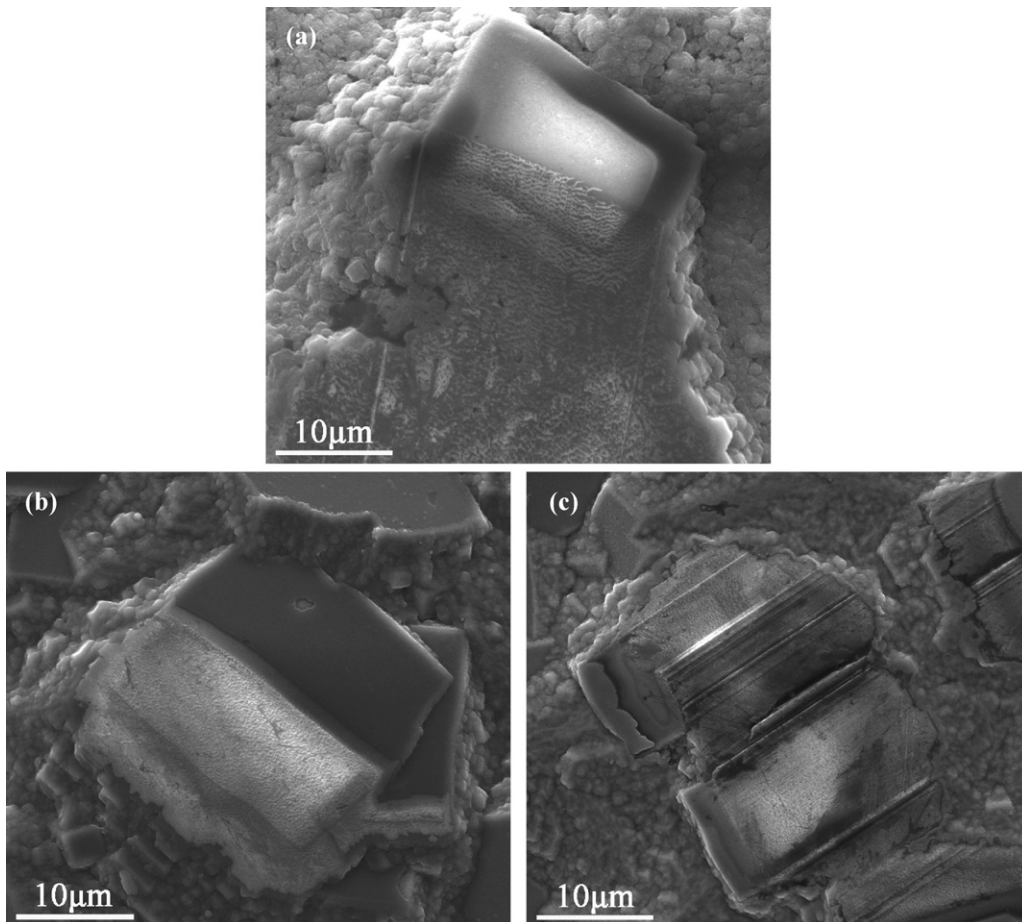


Fig. 8. SEM images of the worn diamond facets for the three as-deposited film samples after wear test: (a) PCD film, (b) PCD/ta-C composite film, (c) PCD/Ti/ta-C composite film.

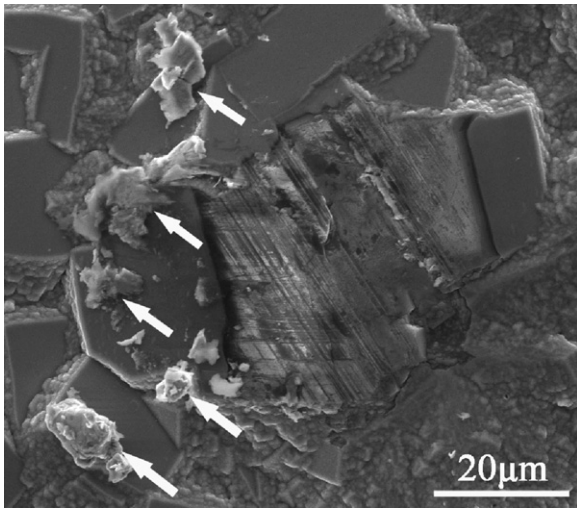


Fig. 9. SEM image of the wear scar for the PCD/Ti/ta-C composite film after the wear test. Some formed debris were distributed on the sides of the wear track.

sliding time prolonged. The reason for this variation is presented in the following discussions.

Typical wear track morphologies of the PCD and PCD/ta-C composite films are illustrated in Fig. 7 for comparison. Severe scratching scars were found on the wear track of the single PCD film sample. On the contrary, the PCD/ta-C composite film sample shows milder and smaller wear scar, indicating better wear resistant property.

To further study the wear mechanism, worn diamond facets of the three samples were characterized by SEM under high magnification, which are shown in Fig. 8. Typical abrasive wear damages were observed on the protruding diamond crystal facets for all the samples. The diamond grain of the PCD film in Fig. 8a shows a large polished surface damage due to its relatively rough surface. In comparison, the diamond grain of the PCD/ta-C composite film in Fig. 8b was only slightly polished at the very top of the protruding diamond face, revealing a better anti-wear property. Apart from polished surface damage, tiny grooves were observed on the worn diamond facets of the PCD/Ti/ta-C composite film in Fig. 8c. These plowing grooves were probably formed by the trapped diamond sub-micro-particles discussed below. It should be noted that there were no crack propagations formed on the abraded diamond grains for all the samples under Hertzian contact pressure during the friction process.

Fig. 9 shows the formed debris on the sides of the wear track of the PCD/Ti/ta-C composite film after the wear test. Small white

debris were dispersed on the surrounding zones. Traces of titanium and carbon were detected by EDS in the wear debris, and a small amount of oxygen was also detected. The reason for formation of these debris was probably due to the low shear strength of the Ti interlayer during deformation comparing to the neighboring PCD and ta-C layers. During prolonged sliding of the two solid surfaces, large volume of the Ti and ta-C layers were worn and peeled off, which were produced as wear debris. The debris were pushed to the side of the track, exposing the bottom diamond asperities. These protruding diamond micro-asperities fractured into sub-micro-particles during friction deformation and trapped at the interface between the surfaces. Then, these particles would adhere on the contacting wear track and act as third-body abrasives between the Si₃N₄ ball and the counterpart diamond surfaces, which caused plowing grooves formed on the worn surface of the film (see Fig. 8c). This also resulted in a higher friction coefficient for the PCD/Ti/ta-C composite film than that of the PCD/ta-C composite film during the steady state shown in Fig. 6. Thus, the addition of Ti interlayer can further reduce the diamond surface roughness, but deteriorate to some extent the tribological performance of the composite film.

Raman measurements were also measured on the worn diamond surface inside the wear track and the deposited surface outside of the wear track, respectively, to analyze the carbon phase transformation [19]. Fig. 10 presents a comparison of Raman spectra for the PCD film and the PCD/ta-C composite film after the wear test. As observed in Fig. 10a, the 'G' band at 1562.7 cm⁻¹ shows the almost identical shape for the worn surface and the deposited surface, implying no phase transformations from diamond to thermodynamically stable graphite during the friction process for single PCD film. In comparison, a notable increase in the 'G' band shown in Fig. 10b for the PCD/ta-C composite film indicated that graphitic transfer layers were generated from the covering ta-C layer due to high shear stresses and flash temperatures in asperities contacts during the friction process [19,27]. The discussed phase transformation leads to the formation of a thin lubricating film between the counterpart contact surfaces. This is an ideal system to reduce friction and wear of the composite film. Especially for the PCD/ta-C composite film, the coarse surface of the PCD film can act as 'storage' for the covering ta-C layer during film formation (Fig. 1a and b). Thus, the ta-C layer can supply a continuous lubricating effect, which resulted in a decrease in the friction coefficient along with duration time. This argument is proved by the friction test results shown in Fig. 6. The discussions presented above demonstrate that deposition of a thick self-lubricating ta-C layer onto the polycrystalline diamond to form PCD/ta-C composite film is an effective method to lower the surface roughness and further improve the tribological performance of the CVD synthesized rough diamond film.

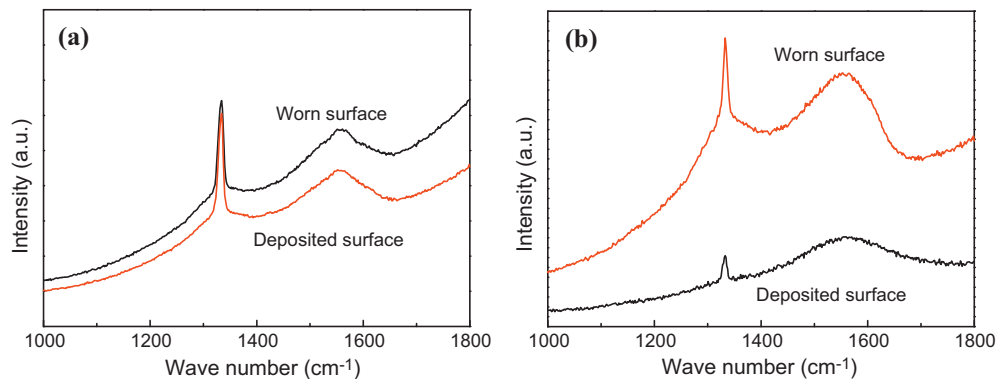


Fig. 10. Raman spectra measured on the worn surface inside the wear track and deposited surface outside of the wear track, respectively, after the ball-on-disk wear test: (a) PCD film, (b) PCD/ta-C composite film.

4. Conclusions

Diamond/tetrahedral amorphous carbon composite films were synthesized by a two-step preparation technique including HFCVD growth for polycrystalline diamond and subsequent FCVA deposition for tetrahedral amorphous carbon. The results indicate that covering a ta-C layer on rough polycrystalline diamond is an effective tool to lower the surface roughness of the polycrystalline diamond film synthesized by CVD method. The wear-resistance of the diamond during the ball-on-disk dry friction test was also enhanced by the self-lubricating effect from the ta-C film due to graphitic phase transformation. The friction coefficients for the composite films were much lower than that of the single PCD film. An extremely low friction coefficient (~ 0.05) was achieved for the PCD/ta-C composite film. The main wear mechanism of the composite films in the dry friction process against ceramic Si_3N_4 ball counterpart was abrasive wear. Moreover, addition of Ti interlayer into the composite film can further reduce the surface roughness of the diamond film. However, the tribological performance of the PCD/Ti/ta-C composite film was deteriorated to some extent due to the low shear strength of the Ti interlayer during deformation.

Acknowledgements

This work was supported by “Key International Cooperation Project, Ministry of Science and Technology, China (grant no. 2006DFB51260)”, the National Natural Science Foundation of China (grant no. 51005218), and the Tribology Science Fund of State Key Laboratory of Tribology in Tsinghua University.

References

- [1] H. Hanyu, S. Kamiya, H. Odagi, Y. Murakami, M. Saka, *Thin Solid Films* 413 (2002) 139.
- [2] F.A. Almeida, A.J.S. Fernandes, R.F. Silva, F.J. Oliveira, *Surf. Coat. Technol.* 201 (2006) 1776.
- [3] J. Yan, K. Syoji, J. Tamaki, *Wear* 255 (2003) 1380.
- [4] S.-T. Lee, Z.D. Lin, X. Jiang, *Mater. Sci. Eng. R* 25 (1999) 123.
- [5] W. Kulisch, C. Popov, S. Boycheva, L. Buforn, G. Favaro, N. Conte, *Diamond Relat. Mater.* 13 (2004) 1997.
- [6] S.J. Askari, G.C. Chen, F. Akhtar, F.X. Lu, *Diamond Relat. Mater.* 17 (2008) 294.
- [7] Q.P. Wei, Z.M. Yu, L. Ma, D.F. Yin, J. Ye, *Appl. Surf. Sci.* 256 (2009) 1322.
- [8] C.Y. Wang, F.L. Zhang, T.C. Kuang, C.L. Chen, *Thin Solid Films* 496 (2006) 698.
- [9] Q.F. Su, J.M. Liu, L.J. Wang, W.M. Shi, Y.B. Xia, *Scripta Mater.* 54 (2006) 1871.
- [10] S.K. Sarangi, A. Chattopadhyay, A.K. Chattopadhyay, *Appl. Surf. Sci.* 254 (2008) 3721.
- [11] F.J.G. Silva, A.J.S. Fernandes, F.M. Costa, A.P.M. Baptista, E. Pereira, *Diamond Relat. Mater.* 13 (2004) 828.
- [12] S.-H. Seo, T.-H. Lee, J.-S. Park, *Diamond Relat. Mater.* 12 (2003) 1670.
- [13] S.A. Catledge, P. Baker, J.T. Tarvin, Y.K. Vohra, *Diamond Relat. Mater.* 9 (2000) 1512.
- [14] M. Vojs, M. Veselý, R. Redhammer, J. Janík, M. Kadlečíková, T. Daniš, M. Marton, M. Michalka, P. Šutta, *Diamond Relat. Mater.* 14 (2005) 613.
- [15] S. Takeuchi, S. Oda, M. Murakawa, *Thin Solid Films* 398–399 (2001) 238.
- [16] Y.-Q. Hou, D.-M. Zhuang, G. Zhang, M.-S. Wu, J.-J. Liu, *Wear* 253 (2002) 711.
- [17] J. Robertson, *Mater. Sci. Eng. R* 37 (2002) 129.
- [18] S. Xu, D. Flynn, B.K. Tay, S. Praver, K.W. Nugent, S.R.P. Silva, Y. Lifshitz, W.I. Milne, *Philos. Mag.* B 76 (1997) 351.
- [19] A.A. Voevodin, A.W. Phelps, J.S. Zabinski, M.S. Donley, *Diamond Relat. Mater.* 5 (1996) 1264.
- [20] M. Nosonovsky, B. Bhushan, *Mater. Sci. Eng. R* 58 (2007) 162.
- [21] A.C. Ferrari, J. Robertson, *Phys. Rev. B* 61 (2000) 14095.
- [22] G. Faggio, M. Marinelli, G. Messina, E. Milani, A. Paoletti, S. Santangelo, A. Tucciarone, G. Verona Rinati, *Diamond Relat. Mater.* 8 (1999) 640.
- [23] X. Yu, X. Zhang, C.-B. Wang, M. Hua, L.-G. Wang, *Vacuum* 75 (2004) 231.
- [24] I.P. Hayward, I.L. Singer, L.E. Seitzman, *Wear* 157 (1992) 215.
- [25] G. Straffellini, P. Scardi, A. Molinari, R. Polini, *Wear* 249 (2001) 461.
- [26] L. Vandenbulcke, M.I. De Barros, *Surf. Coat. Technol.* 146–147 (2001) 417.
- [27] J.E. Field, C.S.J. Pickles, *Diamond Relat. Mater.* 5 (1996) 625.